Theoretical and experimental comparison of gear systems: planetary mechanical transmission and coaxial magnetic gear

Janusz KOŁODZIEJ[ID]*, **Rafał GABOR**[ID], **Marcin KOWOL**[ID], and **Marian ŁUKANISZYN**[ID]

Faculty of Electrical Engineering, Automatic Control and Informatics, Opole University of Technology, Poland

Abstract. Gear systems in today's industry are one of the critical pillars providing power transformation and matching speed and torque to application requirements. Reliability, high efficiency, and low operating costs are desirable due to the prevalence of gearboxes. This paper provides a comparative analysis of selected mechanical and magnetic gears, using a specific example to point out the advantages and disadvantages of contactless power conversion. After determining the essence of the operation of the magnetic gear on the base model, two magnetic gear optimization cases are presented, testifying to the application potential. An analysis of the stress distribution in the area of the teeth of the mechanical gearbox and the most stressed element of the magnetic gear – the modulator, was carried out. The effects of temperature and load on losses were measured and simulated, and ultimately, the efficiency characteristics of the two gears were also compared.

Keywords: planetary gear; magnetic gear; torque density; local force; reliability.

1. INTRODUCTION

Much time has passed since the first mechanical transmissions were used in technical engineering. The experience gained during their operation allowed us to notice the significant advantages and disadvantages of these solutions and to take appropriate remedial steps or give way in some areas, e.g., to hydrostatic or other transmissions [1]. Depending on the specifics of the application, dedicated design solutions for mechanical transmissions were developed, ultimately creating a pervasive and diverse group of devices. The advantages of mechanical gears often mentioned in the literature are high conversion efficiency and torque density. The most frequently mentioned defects in traditional mechanical gears include chipping of the tooth tops, pitting, cracks and breaks of the tooth, cracking of the tooth rim, fatigue chipping of the surface layer of the working surfaces of the teeth, seizing of the active surfaces and others [2–4]. Friction between the cooperating elements of a traditional mechanical transmission is cited as the main reason that negatively affects the service life of the gear [5,6]. Friction in mechanical transmission occurs at the contact of teeth, subject to combined sliding and rolling movements [2,5,7,8]. This physical contact between the gears also generates heat, excessive noise, and vibration and is responsible for forming backlash (Fig. 1) [2, 5, 9, 10]. Statistically, about 60% of failures in mechanical transmissions are caused by damage to the gears. Research conducted on wind energy has shown that mechanical gear failures are one of the main causes of downtime in obtaining energy from off-

shore wind energy [11]. Therefore, it becomes necessary to conduct cyclical inspections and service works for traditional mechanical transmissions, which simultaneously increases the operating costs but prevents unforeseen stops in the production cycle [6, 12, 13].
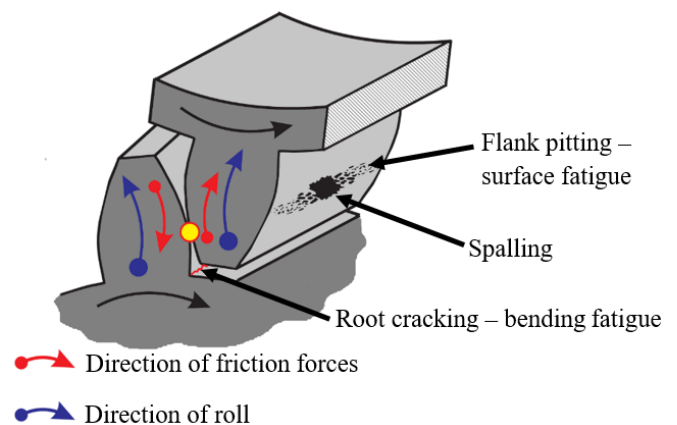
Fig. 1. Mechanics of gear tooth engagement (at point of first contact)

Although mechanical transmissions seem to be described in detail and exhaustively in the literature, they are still an area of research [14, 15]. In their works, the Authors mainly analyze the causes of damage to the mechanical system, bending stresses, contact stresses and perform a reliability analysis. Modern non-invasive methods based on vibroacoustic and neural networks are increasingly used to diagnose gearbox components [3, 16, 17].

The activities undertaken today focus not only on improving the techniques of obtaining environmentally friendly energy but

*e-mail: ja.kolodziej@po.edu.pl

J. Kołodziej, R, Gabor, M. Kowol, and M. Łukaniszyn

also on the search for methods of effective storage and processing. It is crucial to use energy from renewable sources and maximize the efficiency of the energy transformation process. A new transducer capable of replacing the critical mechanical transmission in the process of energy conversion is a magnetic gear (MG) [18]. Modern concepts of magnetic gears containing neodymium magnets allowed for a significant increase in energy conversion efficiency and thus became competitive with mechanical gears, e.g., in WECS (Wind Energy Conversion Systems) [2]. Torque transmission via a magnetic field provides mechanical isolation and eliminates friction between cooperating moving parts. The absence of friction classifies the magnetic gear as a maintenance-free design (the need for lubrication has been eliminated), characterized by natural overload protection. This property, resulting from the lack of connection of the transducer elements, protecting both the drive and the driven system, is an additional advantage, significant in industrial applications susceptible to frequent overloads [19–21].

Currently, available works mainly focus on the construction, principle of operation, design modifications, motion properties, optimization, or other often very detailed research aspects of magnetic gearboxes, mentioning only the critical disadvantages of mechanical gearboxes in general terms. The primary purpose of this paper is to provide a detailed comparison of two contemporary competing converters, discussing the differences in the design and principle of energy transformation, stress distribution, and sources of losses and efficiency. The paper also includes a chapter that presents the results of the magnetic circuit optimization, highlighting the potential of the MG. Can modern magnetic gearboxes successfully compete with mechanical ones regarding operational reliability and operating costs? This paper is one of the few works highlighting essential aspects of both technologies using a specific example.

The structure of the work is as follows: after a short description of the magnetic gear technology, models and prototypes of the compared gears are discussed. Then, the key chapters of the work present an analysis of load distribution and the influence of temperature on torque and losses, and finally, measurements of efficiency characteristics are made.

2. MAGNETIC GEARING CONCEPT

The basis of any magnetic gearbox operation is the magnetic interactions between magnets, both the direct ones and the interactions of harmonic fields modulated through ferromagnetic elements [22]. The critical issue, however, is the size of the area of these interactions and the number of magnets simultaneously involved in the energy transformation. For this reason, some of the magnetic counterparts of mechanical gears do not have application capabilities, but all of them guarantee overload protection and physical separation in the drive system.

A planetary gearbox (PG), which features a compact design and carries a relatively large load, was chosen for the analysis. Using three circulating wheels ensures that the load is evenly distributed over the surfaces of the teeth in contact with each other [23]. Figure 2a shows a schematic of the planetary

gearbox design. The magnetic equivalent of a mechanical planetary gear is shown in Fig. 2b. The key components, the sun wheel, planet wheel, and ring wheel, are equipped with permanent magnets, achieving a relatively high torque density. Huang published one of the first designs of such a gearbox, with performance competitive with mechanical solutions, in 2008 [24]. Other teams researched magnetic planetary gearboxes, the results of which were presented in papers [2, 25, 26]. As simulations have shown, the number of planets in a magnetic planetary gearbox strongly affects the value of transmitted torque. Still, it also forces the evaluation of magnetic couplings. Magnetic planetary gear containing three, four, five, six and nine planets have shown good properties, which have also been confirmed experimentally. However, despite the many advantages, many compo-

(a)

(b)
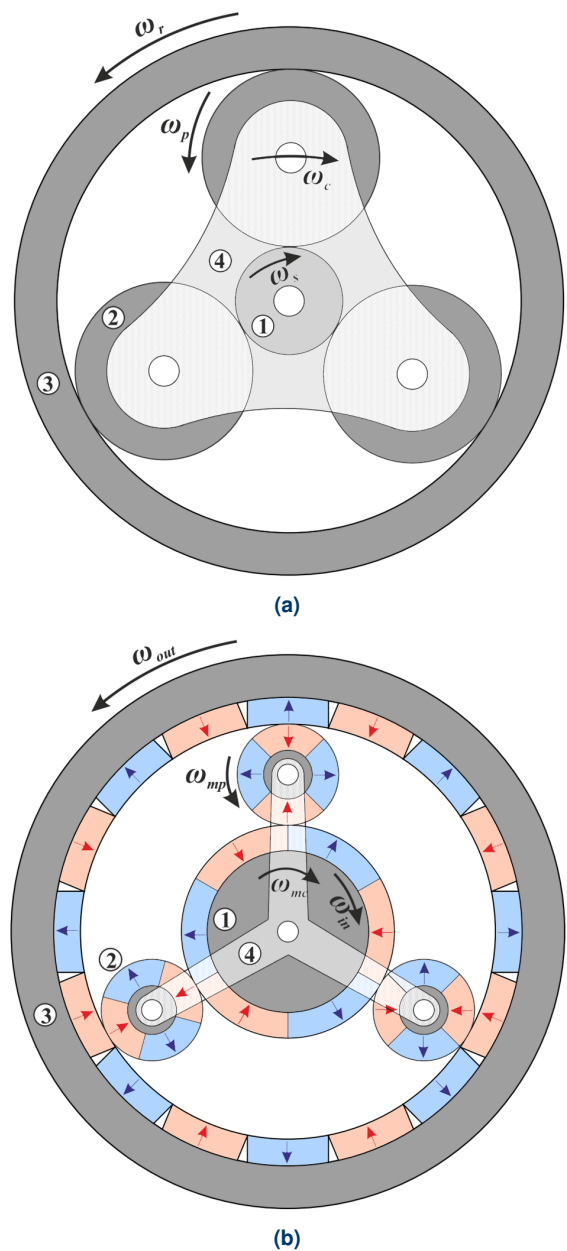
Fig. 2. The key elements (1) sun gear, (2) planet gear, (3) ring gear, (4) planet carrier in (a) mechanical, (b) magnetic gear case

2

Bull. Pol. Acad. Sci. Tech. Sci., vol. 72, no. 5, p. e150334, 2024

nents are troublesome, making it difficult to manufacture, apply, and integrate into permanent magnet electric machines [27].

Magnetic planetary gearing has become competitive with mechanical gearing because it simultaneously engages more magnets to work together. However, can it simultaneously use all magnets while maintaining a relatively simple and robust design? Atallach's work [19] on a new Coaxial Magnetic Gear (CMG) topology, which allows all magnets to participate in the torque transmission process simultaneously, proved to be a breakthrough. The CMG (Fig. 3), which has no mechanical counterpart, is built with concentrically seated inner (1) and outer (3) rotors and a modulator/intermediate ring (2) – which modulates the magnetic field. Many topologies of magnetic gearboxes using flux modulation have been proposed and described in the literature, which differ in design parameters, size and magnetization direction of permanent magnets, gear ratio, etc. [4, 21, 28–31].
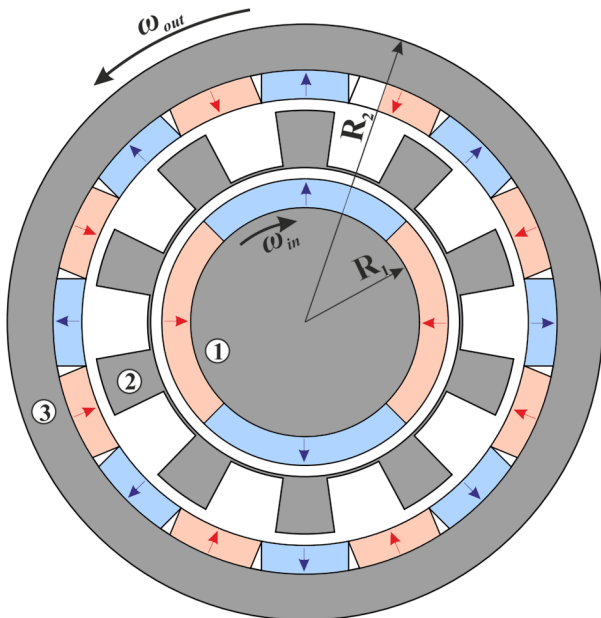

Fig. 3. Coaxial magnetic gear

The CMG was chosen for comparison in the paper because it has no mechanical counterpart and is easier to build than a planetary gearbox. Moreover, adapting to a specific application (e.g., modifying the modulator) is relatively easy while showing some similarities with a planetary gearbox. While reviewing previously published works, no research results showed such a comparison analysis of mechanical planetary gear and CMG combination. In the next chapter, the authors will present the analyzed gearbox variants in detail and make a comparison highlighting the key parameters.

3. GEARS PHYSICAL SPECIFICATION AND MODIFICATIONS

The main feature of each gearbox is its ratio; the gears selected for analysis (PG and CMGs – Base model (BM), Model optimization (Mo. 1)) have identical ratios (G_r = 4:1) and similar

geometric dimensions (Fig. 4). Also significant is the maximum torque value with which the tested converter can be loaded and the torque density ρ_m, defined as the ratio of the maximum torque value (T_{max}) to the volume of the converter (V_p) (1). At the same time, the volume of the transducer is usually taken as the solid resulting from the functional cross-section (e.g., Fig. 2 or 3), ignoring assembly issues, which are dependent on the application.

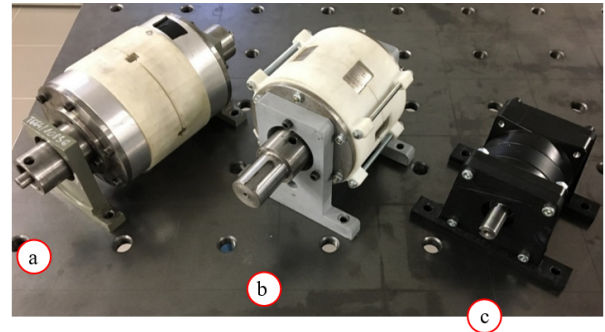$$\rho_m = \frac{T_{\max}}{V_p}. \qquad (1)$$

Fig. 4. Compared gears: (a) CMG BM, (b) CMG Mo. 1, (c) PG

The magnetic gear, the base model in the presented work, cannot fully compete with the mentioned PG due to its performance. It was built to research effective methods of reducing power losses. In this design, the yoke (Fig. 5) was made of a sheet metal package, and the modulator similarly in the form of pins connected by thin magnetic bridges, minimizing losses and torque pulsations [21]. The torque density obtained in this design is not at an impressive level, so to fully illustrate the potential of this design, the authors in the following section proposed two significant modifications to the magnetic circuit, significantly affecting the value and shape of the torque characteristics of the transducer.
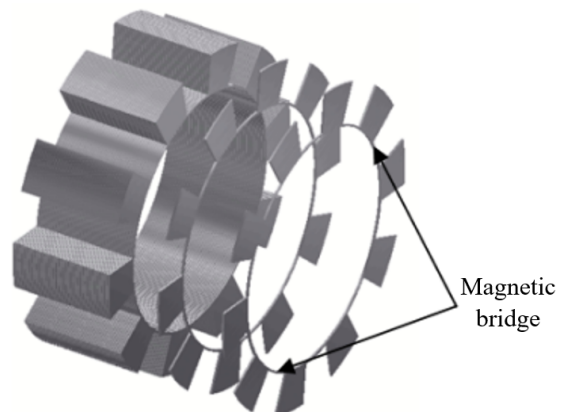

Fig. 5. Modulator pole pieces connected by bridges

In designing the magnetic circuit, it was decided to reduce the number of decision variables, as shown in Fig. 6. Keeping the volume of the converter constant, mainly the geometry of

Bull. Pol. Acad. Sci. Tech. Sci., vol. 72, no. 5, p. e150334, 2024

3

the modulator (M400-50A sheet) and the dimensions of the N35 permanent magnets (NeFe35 – B_r = 1250 mT, H_c = 955 kA/m) were modified. To ensure a gear ratio of 4:1 (for a locked modulator), it was decided to use two pole pairs for the high-speed rotor (p_h), eight pole pairs for the low-speed rotor (p_l), and ten modulator pole pieces (n_s). In further consideration, this combination ($p_l/p_h/n_s \Rightarrow 2/8/10$) is assumed to be constant. The critical geometric parameter of any permanent magnet converter is the thickness of the air gap. In the considered CMG, there are two operating slots. Reducing the thickness of the two slots increases torque values, but in extreme cases, it also causes design problems. Both prototype modifications shown in Fig. 6b and 6c use air gaps reduced to 1 mm. A commercial computing environment was used in the simulations, allowing the calculation of 2D and 3D field models.
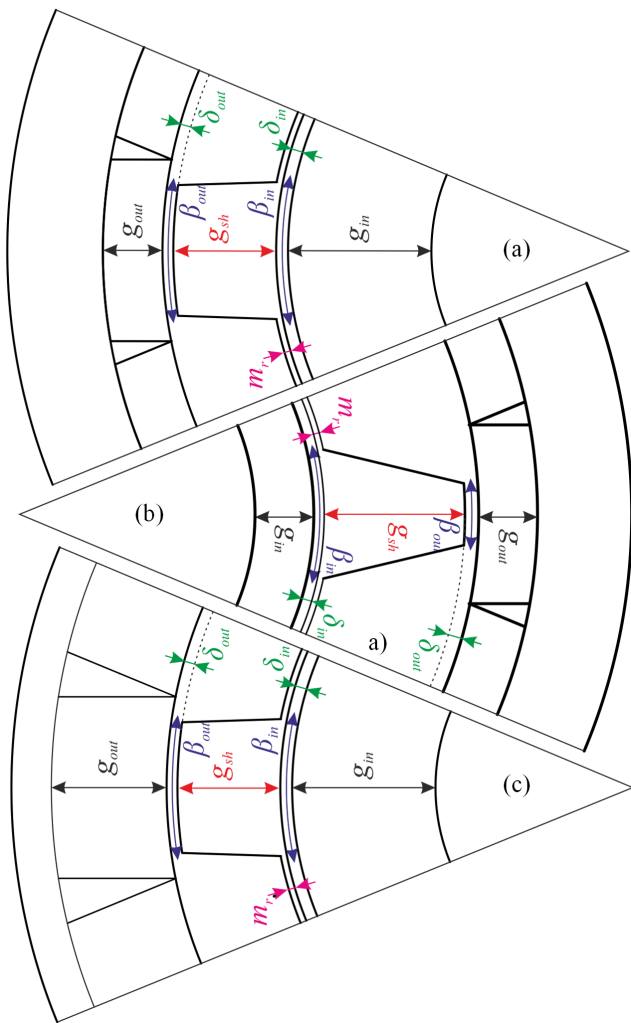
Fig. 6. Geometric parameters of CMG: (a) Base model (BM), (b) Model optimization 1 (Mo. 1), (c) Model optimization 2 (Mo. 2)

A significant disadvantage of electromechanical converters containing high-energy permanent magnets is the tapping torque and torque ripple. The first modification presented in the paper (Mo. 1) concerns the case in which the authors, using the weighted objectives method in the optimization [32,33], focused

on modifying the shape of the modulator pole pieces without changing the dimensions of the magnets (Fig. 6b). The cross-section of the modulator pole pieces resembling a trapezoid is due to the need to reduce harmful torque ripples. In the second modification (Mo. 2), the value of magnetic torque was maximized – it correlates with an apparent increase in the thickness of permanent magnets (Fig. 6c). Detailed information on changes in key geometric parameters is provided in Table 1.

Table 1
Comparison of geometric parameters for CMG models

Parameters	BM	Mo.1	Mo.2
g_{in} [mm]	5	5	12
g_{sh} [mm]	10	12	8.1
g_{out} [mm]	5	5	8.4
m_r [mm]	0.5	0.5	0.5
δ_{in}, δ_{out} [mm]	2	1	1
β_{in} [°]	18	24	22.5
β_{out} [°]	18	8	16.5

The results of the calculations are included in Table 2. The best case (Mo.2) shows a more than twofold increase in maximum torque value while reducing the pulsation value by more than half. Since this gearbox also allows for a 5:1 ratio (for a locked low-speed rotor), the maximum torque and density values obtained are even higher (marked "*"). Most importantly, the modifications presented show the potential of this type of converter, how relatively minor modifications in geometry or material parameters result in significantly improved motion performance of the converter, and its application attractiveness. Each increase in the torque value also directly translates into the force values within the cooperating elements; in the case of a mechanical transmission, this applies to a small meshing area, while in a coaxial magnetic transmission, it concerns the entire modulator area. In the next chapter, the authors will present research not yet published in the literature regarding selected aspects of force analysis and load distribution for the considered gear structures.

Table 2
Comparison of parameters for CMG models (the parameters for a gear ratio 5:1 were marked with *)

Parameters		BM	Mo. 1	Mo. 2	PG
Max Torque [N·m]		15.8/ 19.8*	20.7/25.9*	37.3/46.45*	40
Torque density [(kN·m)/m³]		37.7/ 47.4*	48.8/ 60.8*	87.5/109.2*	363
Torque ripple ratio [%]	ϵ_{in}	6.92	4.38	4.25	–
	ϵ_{out}	0.24	1.17	0.71	–
	ϵ_{mod}	1.35	0.81	0.55	–

4

Bull. Pol. Acad. Sci. Tech. Sci., vol. 72, no. 5, p. e150334, 2024

4. LOAD DISTRIBUTION

In the case of a traditional mechanical planetary gear, the force is focused pointwise on the tooth surface during contact with the second tooth. From the beginning of contact between the mating teeth until the pitch point, the pressure force (F_c) increases as the friction increases. Then, it decreases, reaching 0 when the tooth crosses the last characteristic point (End of contact). Before the pitch point, torque is produced by a tangential force (F_θ) in the direction opposite to the rotation of the drive wheel. The resulting torque counteracts the rotation of the drive wheel, forcing an increase in the torque needed to rotate the sprocket. As a result, the pressure force increases. After exceeding the pitch point, the tangential force takes the same direction as the rotating drive wheel; therefore, less torque is needed to rotate the wheel, and thus, the pressure force in the contact decreases [7].

The forces acting on the teeth (2)–(4) of both the solar gear and the planetary gear retain the same value according to the principle of action and reaction. The force between the contacting teeth (F_{n_SP}) develops perpendicular to the contact surfaces. At the same time, the pressure angle (α) characterizes the angle between the tangential force (circumferential) responsible for transmitting the load and the normal force (Fig. 7) [20,34]. This normal force can be decomposed into a radial force (F_{r_SP}) and a tangential force (F_{θ_SP}), where the subscripts inform the reader between which gears of the planetary gear the force analysis is performed.

$$F_{\theta\_SP} = \frac{2T_S}{D_S}, \tag{2}$$

$$F_{r\_SP} = F_{\theta\_SP} \tan\alpha, \tag{3}$$
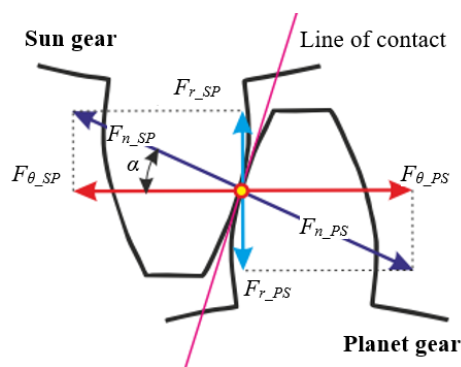
$$F_{n\_SP} = \frac{F_{\theta\_SP}}{\cos\alpha}. \tag{4}$$

Fig. 7. Gear teeth in contact

Magnetic forces (f_{mag}) transmit torque in a magnetic gear, and the most significant values are observed within the modulator. The distribution of forces is described by the divergence of the Maxwell stress tensor $\mathbf{M}$ in the environment – the air gap (5). We obtain a specific force value by integrating it over the volume for the selected element. Considering its particular shape (notched ring, resembling a gear), it is impossible to directly determine the local force acting on one section – the modulator pole piece in analogy to the teeth of a mechanical gear. However, using Gauss's formula, which converts the volume integral into an integral over a closed surface (6), it is possible to decompose the resultant force into the scalar product of the tensor $\mathbf{M}$ and the unit vector $\boldsymbol{n}$ – normal to the integration surface.

$$\vec{f}_{mag} = \nabla \cdot \mathbf{M}, \tag{5}$$

$$\vec{F}_{mag} = \iiint_V (\nu_0 \nabla \cdot \mathbf{M}) \, dV = \nu_0 \oiint_S \mathbf{M} \cdot \boldsymbol{n} \, dS, \tag{6}$$

where ν_0 is reluctivity of vacuum.

The resultant force acting on the selected pole of the modulator (P_i) can be determined by summing the component forces associated with each of the six walls (7) shown in Figure 8. Verification can be carried out based on a comparison of the torque acting on the modulator, calculated in accordance with eq. (8) with measurements [35].

$$\vec{F}_{P_i} = \sum_{j=1}^{6} \vec{F}_{jP_i}, \tag{7}$$

$$T_{mod} = \left(\sum_{i=1}^{n_s} F_{\vartheta P_i} \right) r_{mod}, \tag{8}$$

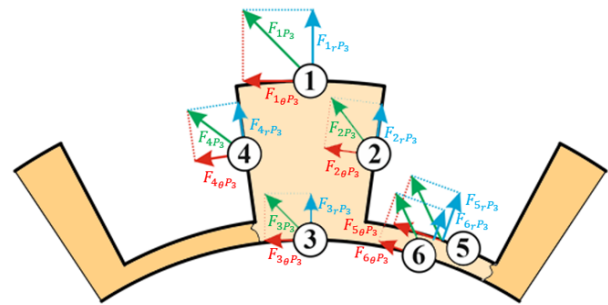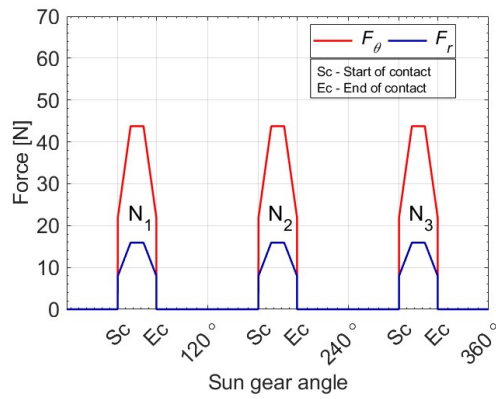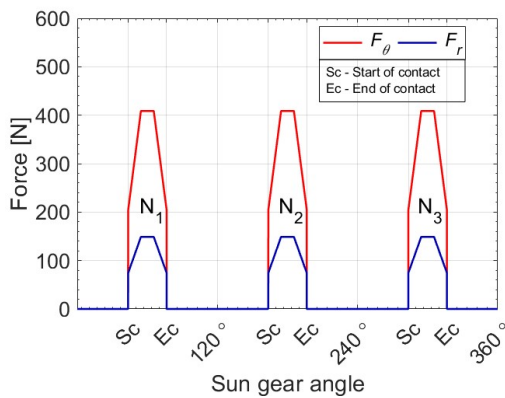where r_{mod} is the modulator guiding ray.

Fig. 8. Local forces on individual walls of pole piece P_3

A graphical interpretation of the variability of the radial and tangential force components for the sun gear of the planetary gear, based on equations (2-4), is presented in Fig. 9, limited to two operating states – at no-load and at load T_l of 12 Nm. Due to the number of planets, each tooth of the sun gear, during its complete revolution, transmits the entire torque three times. The highest observed force value exceeds 400 N and concerns the tangential component for the load T_l, while in the no-load condition, it is approximately ten times smaller. The radial force component in both cases is three times smaller and does not exceed 150 N.

Analogous considerations were carried out for three variants of the concentric magnetic transmission, including working idle and under load T_l. At the no load, the amplitude of the tangential components for the $Mo.$ 1 and $Mo.$ 2 variants is comparable to that of the planetary gear. At the same time, the base model is four times lower (Fig. 11a). Due to the magnetic symmetry of

Bull. Pol. Acad. Sci. Tech. Sci., vol. 72, no. 5, p. e150334, 2024

5

J. Kołodziej, R, Gabor, M. Kowol, and M. Łukaniszyn

Fig. 9. Tangential and radial force components acting on the tooth of the sun gear of the planetary gear (a) at no load, (b) at a load of T_l

the transducers, the radial components completely cancel each other. However, when viewed locally, permanent magnets cause significant radial tensions within the individual poles of the modulator, in extreme cases with an amplitude as much as ten times higher (Fig. 11b).
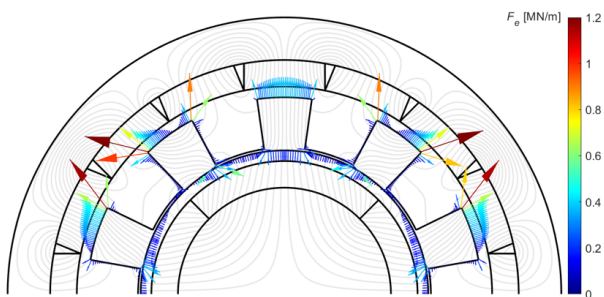

Fig. 10. Flux density lines and local forces on the walls of the CMG at no load
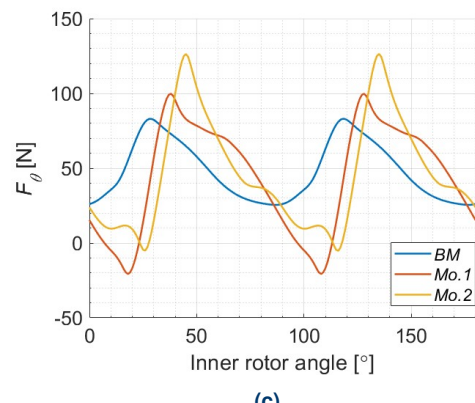
As all poles of the modulator are involved in the torque transfer, the values of the tangential components, just like at no load, are much smaller than in a mechanical planetary gear (Fig. 11c). The radial component of the force acting on the selected pole in all three variants is still relatively high, and its average value
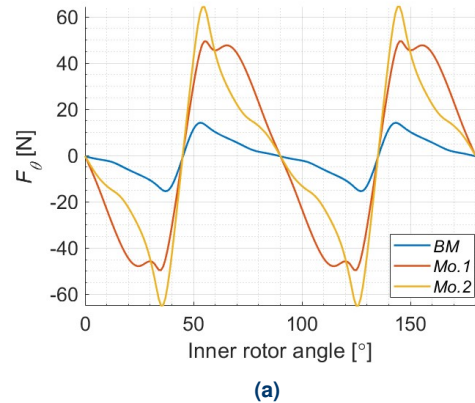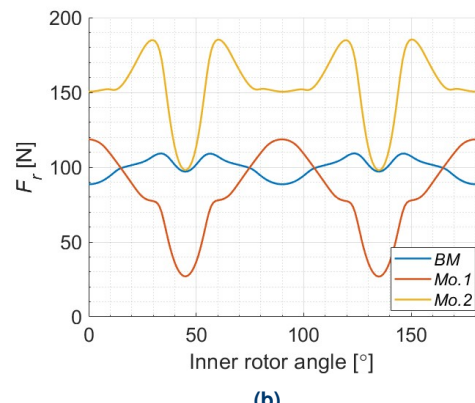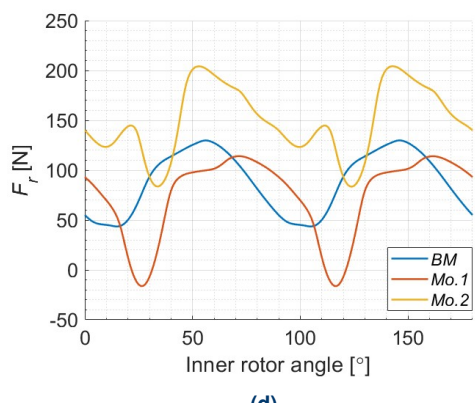

Fig. 11. Variability of tangential and radial force components acting on the selected modulator pole-piece for three CMG variants (BM, $Mo.$ 1, $Mo.$ 2) (a), (b) at no load, (c), (d) at a load of T_l

6

Bull. Pol. Acad. Sci. Tech. Sci., vol. 72, no. 5, p. e150334, 2024

is close to the value in the idle state (Fig. 11d). However, from a global perspective, the transducer is balanced, and the radial tensions cancel out – this applies to all gear designs with integer ratio and magnetic symmetry. Figure 10 shows the distribution of the magnetic field lines in the base model and the distribution of local forces acting on the modulator in the base model (BM) at no load.

Excluding friction is a key issue due to the quality of the transducer operation. Replacing a mechanical gear with a magnetic one can significantly reduce harmful vibrations and noise in the drive system. However, local magnetic interactions with a large amplitude of changes may also be a source of problems. Another important aspect related to energy transformation, present in both mechanical and magnetic transducers, is energy loss. Therefore, in the next chapter, the authors will address the issue of analyzing losses occurring in both types of gears that are considered in operation.

5. LOSS ANALYSIS AND EXPERIMENTAL RESEARCH

Among the many essential properties that characterize modern electromechanical and mechanical converters, the key one, for obvious reasons, is efficiency in energy conversion. This is related to the continuing rise in fuel and energy prices, as well as sustainability and reduction of the environmental impact of fossil fuels. Also key is the size and weight of the converter and, shown in Table 2, the maximum torque and, consequently, the torque density [2].

The authors used measurement stations that were appropriately prepared to conduct experimental research. A stepper motor was used to measure the static torque as a function of the rotation angle of the internal rotor (Fig. 12). For efficiency measurements, the station was equipped with a servo drive and a powder brake to determine the characteristics of the transducers for various loads and precise regulation of the rotational speed.
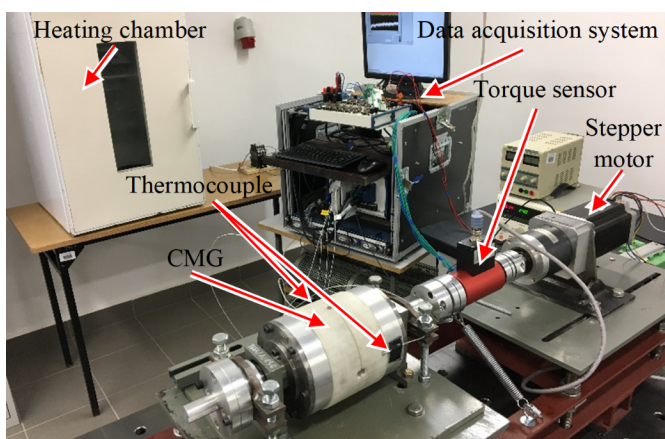

Fig. 12. Measuring station

Calculations were made for a condition classified as a short circuit when the external rotor and modulator are blocked to determine the characteristics of the static torque and its maximum value. In this case, one of the characteristics of magnetic torque

transformation is revealed. Non-destructive measurement verification on the real object is possible only for a magnetic gear since exceeding the maximum torque acting on the converter will not cause damage to the structural components, as in the case of a mechanical planetary gearbox. The results of the calculations obtained from the simulation of the CMG gearbox were compared with the measurements carried out on the test bench, summarized in Fig. 13.
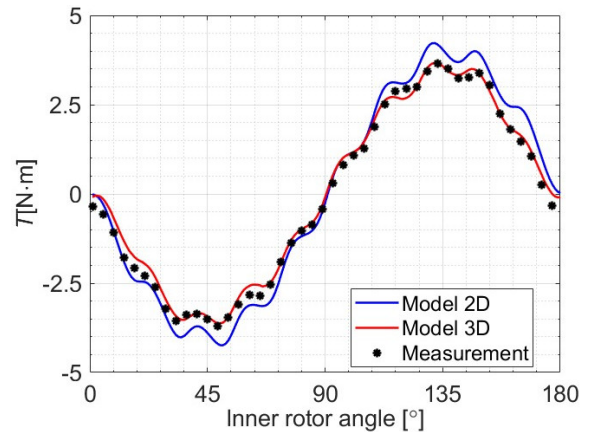

**Fig. 13.** Comparison of magnetic torque characteristics for CMG BM

The operation of the mechanical transmission is influenced by many physical phenomena that affect energy dissipation and deteriorate the condition and operational properties of the transducer. The main power losses occurring in the analyzed planetary gear are of mechanical origin and are caused by friction occurring in lubricated tribological nodes and bearings. These losses depend on the load and increase with the torque transmitted by the transducer [36]. In addition, in a mechanical gearbox, there is a group of non-load-dependent mechanical losses resulting from the rotation of its components. The primary sources of losses resulting from the rotation of elements in a planetary gearbox are viscous drag associated with rotating elements (gears, bearings), pumping of a mixture of grease and air from the space between interlocking teeth (Fig. 14b), and friction-induced losses in bearings. Centrifugal forces of the rotating components cause losses in the bearings of a planetary gearbox [36] and, like losses arising in the gap (windage losses), increase with increasing speed [37].

Each satellite of the planetary gear under consideration is subject to load-dependent and load-independent (viscous) losses. The satellite rotation also causes a centrifugal force that acts on each planetary wheel. These forces cause a load-dependent frictional drag on each satellite, which directly increases the power loss in the converter. The results obtained for the tested PG, shown in Fig. 14a, confirm this trend. The transducer was loaded with a torque (T_l) of 1, 7, and 12 Nm, and the measurements were carried out for the rotational speed range from 0 to 500 rpm on the output shaft (low-speed side) at room temperature (24°C).

The losses in passive magnetic gears are caused by mechanisms similar to those of any machine containing permanent magnets, excluding only the losses associated with the winding.

(a)

(b)
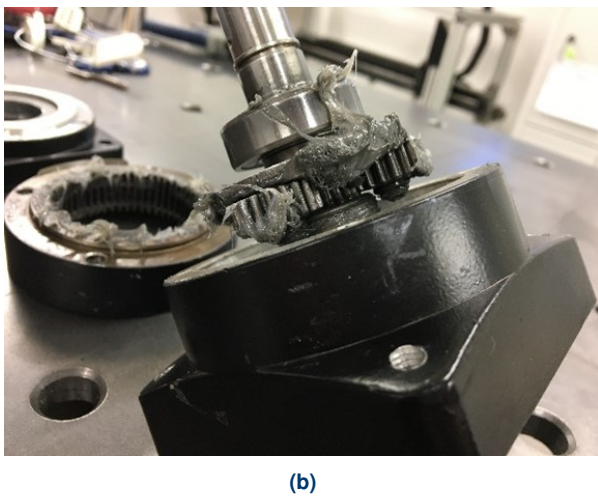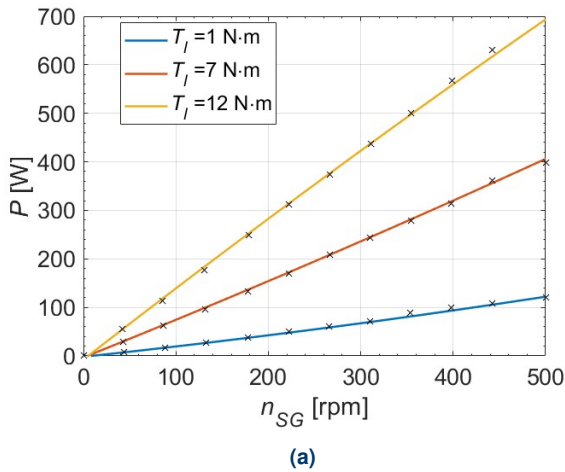
Fig. 14. The PG (a) power as a function of speed for selected loads, (b) disassembled components

Thus, in the overall balance, it is necessary to distinguish between losses of mechanical origin related to friction in bearings, air gaps, and losses of magnetic origin (P_{Fe}) [21]. The identification of losses of magnetic origin was based on the analysis of measurement data, taking into account the binary nature of these losses (9), which depend on the rotational speed, where k_h i k_w is the hysteresis coefficient and eddy current coefficient, respectively.

$$P_{\mathrm{Fe}} = k_h \omega + k_w \omega^2. \tag{9}$$

In a magnetic gearbox, due to the magnetic couplings that occur between the rotors and the stator, it is impossible to make measurements at no load independently for mechanical and magnetic losses. To determine the losses arising in the bearings of the tested structure, the gearbox was decomposed into its components and separate measurements were made. Due to the gearbox low operating speeds and the rotor smooth-walled structure, friction losses in the gaps can be ignored. A detailed analysis of the loss decomposition is presented in the paper [21].

The efficiency of mechanical and magnetic gears is strongly influenced by temperature. For components subject to lubrication, adequate reheating reduces the lubricant viscosity and

improves operating conditions. However, a too-high temperature adversely affects the lubricating properties, friction processes, and wear of gear components. The properties of permanent magnets are mainly related to temperature, so knowledge of the temperature of components under operating conditions is essential for optimal gearbox design.

Magnetic gears are particularly susceptible to high temperatures. The change in the critical parameter of any permanent magnet – the remanence induction – is described by the reversible temperature coefficients of induction provided as 0.12%/°C. This coefficient indicates the percentage change in remanence induction per degree Celsius within the temperature range of 20°C to 80°C. The transducers described in this article are designed to work as structural components of a manipulator in conditions where the operating temperature does not exceed 50°C. However, available papers assume the operation of magnetic gearboxes in environments where the operating temperature is in the range of 150°C [38, 39]. These articles account for the potential for applying magnetic gears in diverse/difficult operating conditions. The torque variation as a function of CMG temperature is shown in Fig. 15 in the form of ranges for three

(a)

(b)
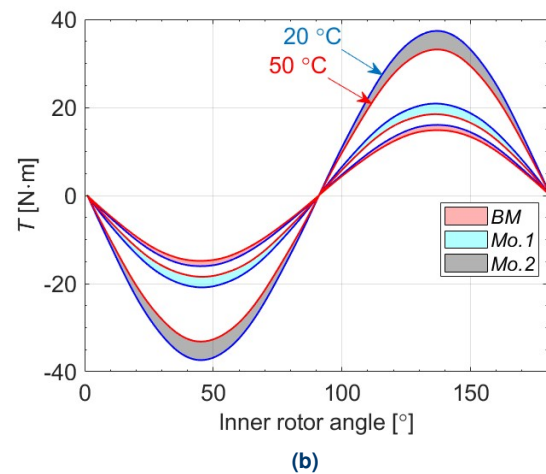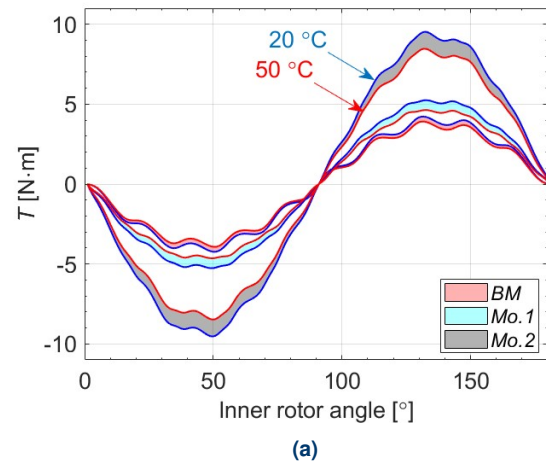
Fig. 15. Angular variation of CMGs torque on (a) high-speed rotor, (b) low-speed rotor, as a function of high-speed rotor rotation angle, for temperatures of 20–50°C

8

Bull. Pol. Acad. Sci. Tech. Sci., vol. 72, no. 5, p. e150334, 2024

models of the CMG converter. The range limits are highlighted in blue at 20°C and red at 50°C. An increase in temperature in the magnetic transducers decreases the achievable torque on its components by about 0.4% for each degree Celsius.

As part of the tests, the gears were placed in a special heating chamber, where the tested transducers were heated to a preset temperature (Fig. 12). Thermocouples, in combination with a dedicated measurement, control, and data acquisition system, were used to control the temperature and reach the set steady state in the CMG. Losses of mechanical origin in the given temperature range decrease in the compared transmitters with increasing temperature (Fig. 16). The main reason for this phenomenon is a decrease in the viscosity of the lubricating medium. This applies to the lubricant in the PG and the lubricating medium in the bearings in both gear cases. For the magnetic gearbox, an increase in temperature also contributes to a reduction in the value of the cogging torque. In a well-designed magnetic gearbox, losses of electromagnetic origin can be practically eliminated. Only the necessary mounting and centering elements remain – the bearings.
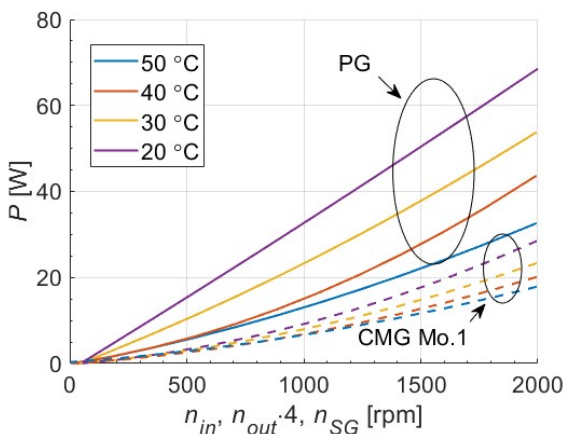

Fig. 16. No load losses for the compared transducers as a function of speed at different temperatures

The most critical parameter of both gears is, of course, the efficiency characteristics. The series of measurements made it possible to plot efficiency characteristics for converters preheated to 30°C (Fig. 17a, 17b). Both the load torque and the speed determine the operating point. The higher value and faster-growing efficiency characteristics of CMG guarantee better operating conditions and efficient energy conversion over a broader range of loads.

6. CONCLUSIONS

Scientific work directly comparing gears derived from two separate technologies are rare. The combination of CMG, which does not have an equivalent in the form of a mechanical transmission, with PG is not accidental. Based on a specific example, the work showed that it is possible to reduce the relatively high point stresses in the PG meshing area from over 400 N almost three times and distribute them evenly around the entire circumference of the CMG. This positively affects the whole machine system, relieving the bearings and reducing vibrations and the risk of secondary damage. Temperature is an often overlooked issue in magnetic gear technology. This work also objectively shows the negative effect of lowering the torque break threshold for the CMG with an increase in temperature of 0.4% for each degree Celsius. The operating temperature is essential for both transducers; it is the reason for limiting the losses related to the viscosity of the lubricant (also in the bearings), but in the case of CMG, it must be taken into account when selecting the class of permanent magnets. Despite significant progress in research on non-contact energy transformation, CMG is still characterized by a significantly lower torque density value, so optimization is the key. As shown in Table 2, however, it is possible to improve the critical parameters of CMG and come closer to the possibilities offered by PG. In the last part of the work, comparing both gears on the basis of efficiency characteristics measurements showed that CMG is a much more advantageous solution in a wide range of loads. The efficiency of the magnetic gear in the
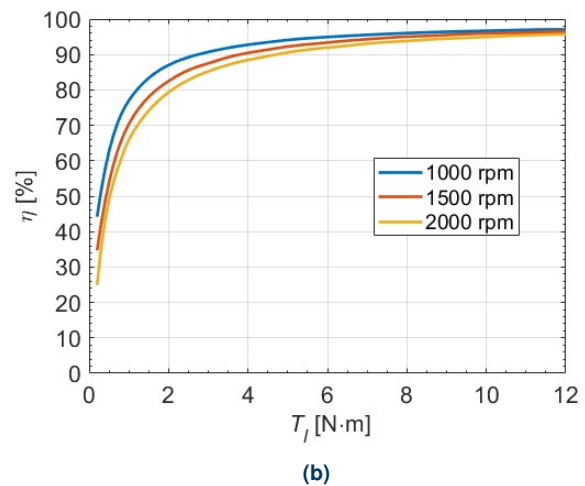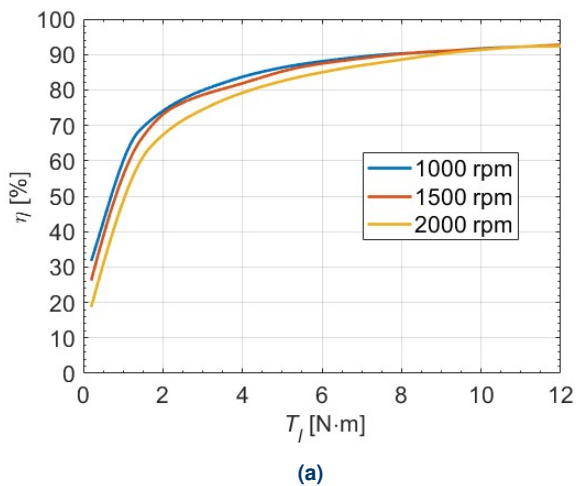

(a)

(b)

Fig. 17. Efficiency characteristics for (a) PG and (b) CMG BM

Bull. Pol. Acad. Sci. Tech. Sci., vol. 72, no. 5, p. e150334, 2024

9

range of small loads that do not exceed 20% of the rated torque is more than 15% higher, and the final efficiency reaches an impressive 97% for a low-power converter.

REFERENCES

[1] P. Bury, M. Stosiak, K. Urbanowicz, A. Kodura, M. Kubrak, and A. Malesińska, "A case study of open-and closed-loop control of hydrostatic transmission with proportional valve start-up process," *Energies*, vol. 15, no. 5, p. 1860, 2022, doi: 10.3390/en15051860.

[2] G. Ruiz-Ponce, M.A. Arjona, C. Hernandez, and R. Escarela-Perez, "A review of magnetic gear technologies used in mechanical power transmission," *Energies*, vol. 16, no. 4, p. 1721, 2023, doi: 10.3390/EN16041721.

[3] V. Sharma and A. Parey, "A review of gear fault diagnosis using various condition indicators," *Procedia Eng.*, vol. 144, pp. 253–263, 2016, doi: 10.1016/j.proeng.2016.05.131.

[4] J.X. Shen, H.Y. Li, H. Hao, and M.J. Jin, "A coaxial magnetic gear with consequent-pole rotors," *IEEE Tran. Energy Convers.*, vol. 32, no. 1, pp. 267–275, 2017, doi: 10.1109/TEC.2016.2609338.

[5] A. Kahraman and S. Li, "Friction in gears," in *Encyclopedia of Tribology*, Springer, Boston, 2013, pp. 1315–1322, doi: 10.1007/978-0-387-92897-5_675.

[6] Z. Li and K. Mao, "Frictional effects on gear tooth contact analysis," *Adv. Tribol.*, vol. 2013, p. 181048, 2013, doi: 10.1155/2013/181048.

[7] S.M. Bae, K.J. Seo, and D.E. Kim, "Effect of friction on the contact stress of a coated polymer gear," *Friction*, vol. 8, no. 6, pp. 1169–1177, 2020, doi: 10.1007/s40544-020-0363-6.

[8] R. Cieślicki and M. Karpenko, "An investigation of the impact of pump deformations on circumferential gap height as a factor influencing volumetric efficiency of external gear pumps," *Transport*, vol. 37, no. 6, p. 373–382, 2022, doi: 10.3846/transport.2022.18331.

[9] J.I. Lee *et al.*, "Design and analysis of the coaxial magnetic gear considering the electromagnetic performance and mechanical stress," *IEEE Trans. Appl. Superconduct.*, vol. 30, no. 4, pp. 1–5, 2020, doi: 10.1109/TASC.2020.2968267.

[10] M. Stosiak, "The impact of hydraulic systems on the human being and the environment," *J. Theor. Appl. Mech.*, vol. 53, no. 2, pp. 409–420, 2015, doi: 10.15632/jtam-pl.53.2.409.

[11] H. Li, W. Peng, C.G. Huang, and C.G. Soares, "Failure rate assessment for onshore and floating offshore wind turbines," *J. Marine Sci. Eng.*, vol. 10, no. 12, p. 1965, 2022, doi: 10.3390/jmse10121965.

[12] Y. Kong, T. Wang, and F. Chu, "Meshing frequency modulation assisted empirical wavelet transform for fault diagnosis of wind turbine planetary ring gear," *Renew. Energy*, vol. 132, pp. 1373–1388, 2019, doi: 10.1016/j.renene.2018.09.027.

[13] J. Shen, L. Zhang, and N. Hu, "Fault diagnosis of planet gear using continuous vibration separation and minimum entropy deconvolution," *Appl. Sci.*, vol. 10, no. 22, p. 8062, 2020, doi: 10.3390/app10228062.

[14] M. Duchemin and V. Collée, "Profile optimization of the teeth of the double rackand-pinion gear mechanism in the mce-5 vcri," in *International Gear Conference 2014*, 2014, doi: 10.1533/9781782421955.55.

[15] S. Lagutin, A. Sandler, and E. Gudov, "Actual issues of design and production of advanced worm gears," *Mech. Mach. Sci.*, vol. 51, p. 139–166, 2018, doi: 10.1007/978-3-319-60399-5_7.

[16] M. Nie and L. Wang, "Review of condition monitoring and fault diagnosis technologies for wind turbine gearbox," *Procedia CIRP – 2nd International Through-life Engineering Services Conference*, vol. 11, pp. 287–290, 2013, doi: 10.1016/j.procir.2013.07.018.

[17] P. Pawlik, "The use of the acoustic signal to diagnose machines operated under variable load," *Arch. Acoust.*, vol. 45, no. 2, pp. 263–270, 2020.

[18] H. Faus, "Magnet gearing," U.S. Patent US2 243 555A, Aug. 1941.

[19] K. Atallah and D. Howe, "A novel high-performance magnetic gear," *IEEE Trans. Magn.*, vol. 37, no. 4, pp. 2844–2846, 2001, doi: 10.1109/20.951324.

[20] S. Gerber, "Evaluation and design aspects of magnetic gears and magnetically geared electrical machines," Ph.D. dissertation, Stellenbosch University, 2015.

[21] M. Kowol, J. Kolodziej, M. Jagiela, and M. Lukaniszyn, "Impact of modulator designs and materials on efficiency and losses in radial passive magnetic gear," *IEEE Trans. Energy Convers.*, vol. 34, no. 1, pp. 147–154, 2019, doi: 10.1109/TEC.2018.2862462.

[22] P.M. Tlali, R.J. Wang, and S. Gerber, "Magnetic gear technologies: A review," in *2014 International Conference on Electrical Machines (ICEM)*, 2014, pp. 544–550, doi: 10.1109/ICELMACH.2014.6960233.

[23] G. Balbayev and M. Ceccarelli, "Design and characterization of a new planetary gear box," in *New Advances in Mechanisms, Transmissions and Applications*, vol. 17, Dordrecht: Springer Netherlands, 2014, pp. 91–98, doi: 10.1007/978-94-007-7485-8_12.

[24] C.C. Huang, M.C. Tsai, D.G. Dorrell, and B.J. Lin, "Development of a magnetic planetary gearbox," *IEEE Trans. Magn.*, vol. 44, no. 3, pp. 403–412, 2008, doi: 10.1109/TMAG.2007.914665.

[25] N. Niguchi and K. Hirata, "Transmission torque analysis of a novel magnetic planetary gear employing 3-d fem," *IEEE Trans. Magn.*, vol. 48, no. 2, pp. 1043–1046, 2012, doi: 10.1109/TMAG.2011.2173662.

[26] M.C. Tsai and C.C. Huang, "Development of a variable-inertia device with a magnetic planetary gearbox," *IEEE/ASME Trans. Mechatron.*, vol. 16, no. 6, pp. 1120–1128, 2011, doi: 10.1109/TMECH.2010.2077679.

[27] T.V. Frandsen *et al.*, "Motor integrated permanent magnet gear in a battery electrical vehicle," *IEEE Trans Ind. Appl.*, vol. 51, no. 2, pp. 1516–1525, 2015, doi: 10.1109/TIA.2014.2360016.

[28] P.O. Rasmussen, T.O. Andersen, F.T. Jørgensen, and O. Nielsen, "Development of a high-performance magnetic gear," *IEEE Trans Ind. Appl.*, vol. 41, no. 3, pp. 764–770, 2005, doi: 10.1109/TIA.2005.847319.

[29] J. Rens, R. Clark, S. Calverley, K. Atallah, and D. Howe, "Design, analysis and realization of a novel magnetic harmonic gear," in *Proceedings of the 2008 International Conference on Electrical Machines, ICEM'08*, 2008, doi: 10.1109/ICELMACH.2008.4800163.

[30] K.K. Uppalapati, M.D. Calvin, J.D. Wright, J. Pitchard, W.B. Williams, and J.Z. Bird, "A magnetic gearbox with an active region torque density of 239 n·m/l," *IEEE Trans Ind. Appl.*,

10

Bull. Pol. Acad. Sci. Tech. Sci., vol. 72, no. 5, p. e150334, 2024

vol. 54, no. 2, pp. 1331–1338, 2018, doi: 10.1109/TIA.2017.2779418.

[31] X. Liu, D. Chen, L. Yi, C. Zhang, and M. Wang, "Comparison and analysis of magnetic-geared permanent magnet electrical machine at no-load," *Arch. Electr. Eng.*, vol. 63, no. 4, pp. 683–692, 2014.

[32] Ł. Knypiński, "A novel hybrid cuckoo search algorithm for optimization of a line-start pm synchronous motor," *Bull. Pol. Acad. Sci. Tech. Sci.*, vol. 71, no. 1, p. e144586, 2023.

[33] E. Zitzler, "Evolutionary algorithms for multiobjective optimization: Methods and applications," Ph.D. dissertation, Swiss Federal Institute of Technology Zurich, 1999.

[34] P. Strojny, "Impact of gear rim narrowing angle on the temperature and sound pressure of beveloid gear pair made of polymeric materials," *Bull. Pol. Acad. Sci. Tech. Sci.*, vol. 69, no. 5, p. e138818, 2021.

[35] M. Kowol, J. Kołodziej, R. Gabor, M. Łukaniszyn, and M. Jagieła, "On-load characteristics of local and global forces in co-axial magnetic gear with reference to additively manufac-

tured parts of modulator," *Energies*, vol. 13, no. 12, p. 3169, 2020, doi: 10.3390/en13123169.

[36] A. Kahraman, D.R. Hilty, and A. Singh, "An experimental investigation of spin power losses of a planetary gear set," *Mech. Mach. Theory*, vol. 86, pp. 48–61, 2015, doi: 10.1016/j.mechmachtheory.2014.12.003.

[37] Y. Wang, W. Yang, X. Tang, X. Lin, and Z. He, "Power flow and efficiency analysis of high-speed heavy load herringbone planetary transmission using a hypergraph-based method," *Appl. Sci.*, vol. 10, no. 17, p. 5849, 2020, doi: 10.3390/app10175849.

[38] M.C. Gardner, B. Praslicka, M. Johnson, and H.A. Toliyat, "Optimization of coaxial magnetic gear design and magnet material grade at different temperatures and gear ratios," *IEEE Trans. Energy Convers.*, vol. 36, no. 3, pp. 2493–2501, 2021, doi: 10.1109/TEC.2021.3054806.

[39] T.F. Tallerico, Z.A. Cameron, and J.J. Scheidler, "Design of a magnetic gear for nasa's vertical lift quadrotor concept vehicle," in *AIAA Propulsion and Energy 2019 Forum and Exposition*, 2019, doi: 10.2514/6.2019-4477.

Bull. Pol. Acad. Sci. Tech. Sci., vol. 72, no. 5, p. e150334, 2024

11